ELSEVIER

Journal of Organometallic Chemistry 642 (2002) 148–155

Journal of Organometallic Chemistry

www.elsevier.com/locate/jorganchem

Solid-state structures of persubstituted titanocene chlorides bridged with long aliphatic *ansa*-chains

Michal Horáček [a], Petr Štěpnička [b], Karla Fejfarová [b], Róbert Gyepes [b], Ivana Císařová [b], Jiří Kubišta [a], Karel Mach [a,*]

[a] *J. Heyrovský Institute of Physical Chemistry, Academy of Sciences of the Czech Republic, Dolejškova 3, 182 23 Prague 8, Czech Republic*
[b] *Department of Inorganic Chemistry, Charles University, Hlavova 2030, 128 40 Prague 2, Czech Republic*

Received 2 July 2001; received in revised form 22 August 2001; accepted 10 September 2001

Abstract

A series of three *ansa*-titanocene monochlorides containing η^5-tetramethylcyclopentadienyl ligands bridged by five- or eight-membered aliphatic chains were prepared via reduction of the corresponding dichlorides with half molar equivalent of magnesium and characterized by spectral methods. The solid-state structures of the monochloride complexes *ansa*-[TiCl{η^5:η^5-$C_5Me_4CH(Me)CH_2CH_2CH(Me)CH(Me)C_5Me_4$}] (**1a**) and *ansa*-[TiCl{η^5:η^5-$C_5Me_4(CH_2)_3CH(Me)CH(Me)CH{=}CHCH_2C_5Me_4$}] (**4a**), and of the bridge-unsaturated titanocene dichloride complex *ansa*-[$TiCl_2${η^5:η^5-$C_5Me_4CH_2CH{=}CH(CH_2)_5C_5Me_4$}] (**3**) were determined by single-crystal X-ray diffraction. All the compounds show bent metallocene structures with the *ansa*-chain situated in a side position with respect to Cg, Ti, Cg (Cg = centroid of the cyclopentadienyl ligand) plane. Angles subtended by the least-squares planes of the cyclopentadienyl rings and conformation of the *ansa*-chains indicates the absence of steric strain in the metallocene framework. © 2002 Elsevier Science B.V. All rights reserved.

Keywords: Titanium; Titanocene; Permethyltitanocene; *ansa*-Carbon chain; Crystal structures; ESR spectroscopy

1. Introduction

Conformational rigidity of Group 4 *ansa*-metallocene complexes decreases with an increasing length of the bridging *ansa*-chain. A low activation energy of rotational reorientation of the cyclopentadienyl ligands in long-chain *ansa*-complexes can allow the two configurations of a metallocene catalytic centre to interchange during the course of catalytic polymerization of 1-alkenes [1]. Hence, such catalysts produce polymers with more or less regular structures of alternating atactic and isotactic sequences whose lengths vary with the reaction temperature [2]. The use of *ansa*-titanocene or *ansa*-zirconocene compounds with long sp^3 carbon chain bridges in alkene polymerization has not yet been investigated in detail, the attention being paid to *ansa*-compounds with more rigid mono- and diatomic bridges or C_4-bridges [1,3] derived from biphenyl [4], 9,10-ethanoanthracene [5] or binaphthyl [6].

The synthesis of *ansa*-metallocene dichlorides relying on a metathetical reaction between dilithiobis(cyclopentadienyl)alkanes and MCl_4 (M = Ti, Zr, Hf) usually gives only poor yields for compounds with long *ansa*-chains. For instance, *ansa*-bis(indenyl)zirconium dichloride with dodecane-1,12-diyl bridge was obtained as *rac*- and *meso*-forms in 15 and 11% yields by the metathesis of 1,12-bis(lithioindenyl)dodecane with $ZrCl_4$ in THF and toluene, respectively [7]. Recently, *ansa*-bis(cyclopentadienyl)zirconium dichlorides with nonane-1,9-diyl and dodecane-1,12-diyl bridges were obtained by the same method in 7 and 18% yields, respectively [8]. Among the other *ansa*-metallocenes prepared by the metathetical approach, *ansa*-titanocene dichlorides with trimethylene bridge were obtained in 11% yield [9] and those with the $SiMe_2CH_2CH_2SiMe_2$ chain in 23% yield [10].

We have recently discovered a novel approach which provides long-chain *ansa*-titanocene dichlorides in excellent yields. It is based on the reduction of ω-alkenyl titanocene dichlorides with magnesium to give ring-

* Corresponding author. Tel.: +420-2-858-5367; fax: +420-2-858-2307.
E-mail address: mach@jh-inst.cas.cz (K. Mach).

PII: S0022-328X(01)01287-6

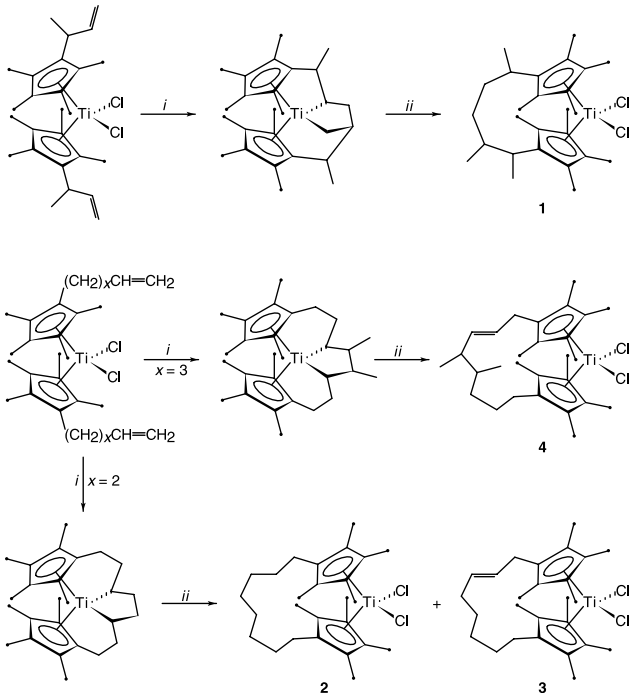

Scheme 1. Novel synthesis of *ansa*-titanocene dichlorides with long *ansa*-chains. Legend: (i) Mg/THF ($-MgCl_2$); (ii) 2HCl.

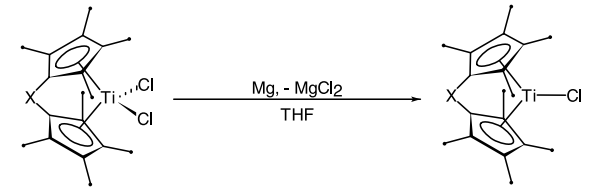

Scheme 2. Preparation of *ansa*-titanocene monochlorides.

tethered titanacyclopentane derivatives, the products of oxidative cycloaddition of the terminal double bonds across a titanium(II) intermediate. These are subsequently opened with HCl, thus yielding the corresponding titanocene dichlorides as shown in Scheme 1 [11]. The structures of *ansa*-complexes **1**–**4** were determined from ^{1}H- and ^{13}C-NMR spectra and, in the case of complex **2**, further corroborated by single-crystal X-ray diffraction [11]. Similar ring-tethered zircona- and hafnacyclopentane derivatives were synthesized by Erker and coworkers [12] in a modified procedure; however, the opening of their metallacyclopentane moieties by acidolysis was not carried out.

As a continuation of our work, we report the preparation of *ansa*-titanocene monochlorides from compounds **1**, **2**, and **4** (denoted as **1a**, **2a**, and **4a**) and solid-state structures of compounds **3**, **1a** and **4a** in order to visualize the conformation of the *ansa*-chains and their influence on the titanocene framework.

2. Results and discussion

Compounds **1**, **2**, and **4** are reduced in THF solutions by magnesium turnings to give the corresponding monochlorides **1a**, **2a**, and **4a** (Scheme 2). As the reaction is rather slow with a stoichiometric titanocene–Mg ratio, a small surplus of Mg was used and the reduction was stopped when the reaction mixture turned turquoise due to the formation of the monochlorides. Small amounts of reaction byproducts resulting from a subsequent reduction of the *ansa*-titanocene monochlorides were removed by extraction with hexane.

The turquoise *ansa*-titanocene monochlorides **1a**, **2a** and **4a** are monomeric and do not coordinate THF. Such behaviour is common for highly substituted titanocene monohalides [13]. The titanium atom in the monochloride complexes has d^1 configuration and, hence, the compounds are paramagnetic, displaying typical highly anisotropic ESR spectra in frozen toluene solution. A comparison of their ESR parameters with the data reported for similar highly substituted titanocene chlorides is given in Table 1. The anisotropy of the g-tensor reflects the extent of π-donation of the σ-substituent to the empty b_2 orbital of the titanocene moiety [14]. For the chloride ligand, a slight increase in

Table 1
ESR parameters for *ansa*-titanocene chlorides **1a**, **2a**, **4a** and some fully substituted titanocene chlorides [$TiCl(\eta^5\text{-}C_5Me_4R)_2$] in toluene solution (22 °C) and in toluene glass (−140 °C)

Compound	g_{iso}	ΔH (G)	g_{av} [a]	g_1	g_2	g_3	References
1a	1.948	23	1.948	1.998	1.982	1.865	This work
2a	1.952	16	1.954	1.998	1.983	1.882	This work
4a	1.955	10	1.958	1.999	1.982	1.893	This work
R = H	1.964	12	1.965	2.000	1.985	1.910	[13]
R = Me	1.957	34	1.956	1.999	1.984	1.889	[13,14]
R = Ph	1.954	10	1.954	1.999	1.982	1.882	[15]
R = $SiMe_3$	1.953	14	1.958	1.999	1.982	1.893	[16]

[a] Average value: $g_{av} = 1/3(g_1+g_2+g_3)$.

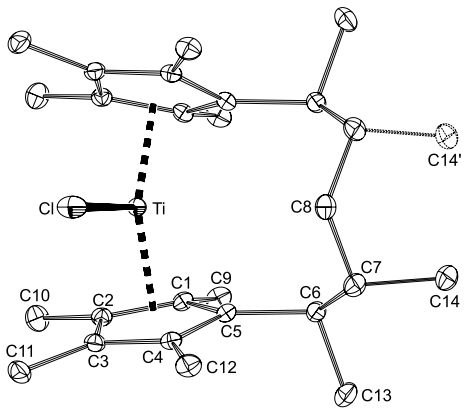

Fig. 1. Molecular structure of **1a** (30% probability ellipsoids) with the atom numbering scheme. The non-labelled atoms are generated by the symmetry operation (x, $1/2-y$, z). The second position of the disordered C(14) atom is denoted by dashed lines. For clarity, hydrogen atoms are omitted.

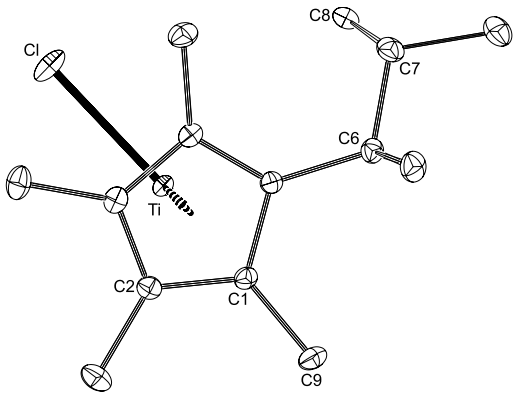

Fig. 2. Structure of **1a** viewed along the Cg–Cg′ line.

Table 2
Selected bond lengths (Å) and bond angles (°) for **1a**

Bond lengths			
Ti–Cg [a]	2.057(1)	Ti–Cl	2.3750(6)
Ti–C(1)	2.389(1)	Ti–C(2)	2.373(1)
Ti–C(3)	2.399(1)	Ti–C(4)	2.403(1)
Ti–C(5)	2.370(1)	C(5)–C(6)	1.518(2)
C(6)–C(7)	1.544(2)	C(7)–C(8)	1.532(2)
C(6)–C(13)	1.536(2)	C(7)–C(14)	1.568(3)
C_{ring}–C_{Me}	1.499(2)–1.504(2)		
Bond angles			
Cg–Ti–Cg′ [b]	139.1(2)	Cl–Ti–Cg	110.4(1)
C(5)–C(6)–C(7)	116.6(1)	C(6)–C(7)–C(8)	117.2(1)
C(7)–C(8)–C(7′) [b]	118.5(2)	ϕ [c]	37.4(2)

[a] Cg denotes the centroid of the C(1–5) cyclopentadienyl ring atoms; Cg′ is the centroid of the symmetry generated ring.

[b] Symmetry transformation used to generate equivalent positions: x, $1/2-y$, z.

[c] Dihedral angle between the least-squares cyclopentadienyl planes.

the anisotropy in the order $[TiCl(\eta^5\text{-}C_5HMe_4)_2] < [TiCl(\eta^5\text{-}C_5Me_5)_2] \sim [TiCl(\eta^5\text{-}C_5Me_4SiMe_3)_2] \sim [TiCl(\eta^5\text{-}C_5Me_4Ph)_2] \sim$ **4a** $\sim$ **2a** $<$ **1a** as indicated by g_{iso}, g_3 and g_{av} values may be accounted for a change of the energy gap between the $1a_1$ orbital occupied by the unpaired electron and b_2 orbital which results from a change in the angle subtended by the cyclopentadienyl-ring planes [17].

Electronic absorption spectra of the monochloride complexes are practically identical because the $1a_1 \rightarrow b_2$ transition is not observable in the measured range of 340–2000 nm; it should be observed at longer wavelengths ($\lambda > 2000$ nm) [13–16].

The *ansa*-link between the cyclopentadienyl rings strongly affects the mass spectra fragmentation upon electron impact. The molecular radical cations $M^{+\bullet}$ are far the most abundant ions in EIMS spectra of **1a** and **4a** whereas in the case of unbridged analogues, the molecular ions are usually accompanied by moderately abundant $[M-HCl]^+$, and $[M-Cp]^+$ fragment ions [15,16]. Compound **3** behaves similarly, eliminating easily the first chlorine atom but not the second one.

2.1. Crystal structures of *1a*, *4a*, and *3*

The solid-state structures of compounds **1a** and **4a** have been determined by X-ray single-crystal diffraction. The crystal structure of **2a** was not investigated because the conformation of the chain in **2** is already known [11]. No attempt has been made to prepare compound **3a** because of lack of pure compound **3**. Nevertheless, several X-ray quality crystals of the dichloride complex **3** were obtained which allowed us to determine its crystal structure and compare the conformation of its unsaturated eight-membered *ansa*-chain with the saturated chain in **2** and the unsaturated *ansa*-chain in **4a**.

Compound **1a** is symmetric with respect to the plane defined by the Ti, Cl, and C(8) atoms because the C(14) atom is disordered over two equally populated positions (C(14) and C(14′); Fig. 1). The cyclopentadienyl ligands are bent approximately in the Cl–C(1) direction with the C(1) atom at the hinge side of the titanocene framework (see a view along the Cg–Cg′ direction in Fig. 2). The C(1) atom is deviated from the plane defined by Cg (Cg denotes cyclopentadienyl-ring centroid), Ti, and Cg′ by only 0.09(5) Å while the Cl atom is disposed by 0.18(7) Å from the plane in the opposite direction. The C(9) atoms which are only 0.10(8) Å away from this plane deviate from the least-squares cyclopentadienyl plane by as much as 0.454(3) Å whereas the C(6) atom of the *ansa*-chain by only 0.190(3) Å and the carbon atoms of other methyl groups by only 0.057–0.121(3) Å, all outwards the titanium atom. The *ansa*-chain is situated in a side position which allows the arrangement of the sp^3 car-

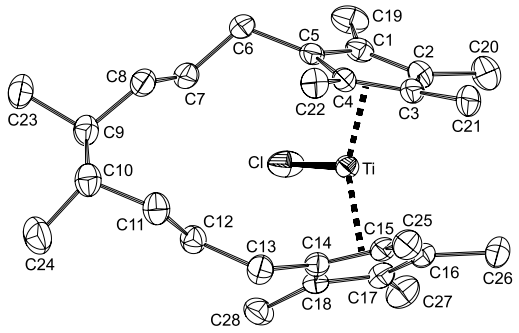

Fig. 3. Molecular structure of **4a** (30% probability ellipsoids) showing the atom numbering scheme. For clarity, all hydrogen atoms are omitted.

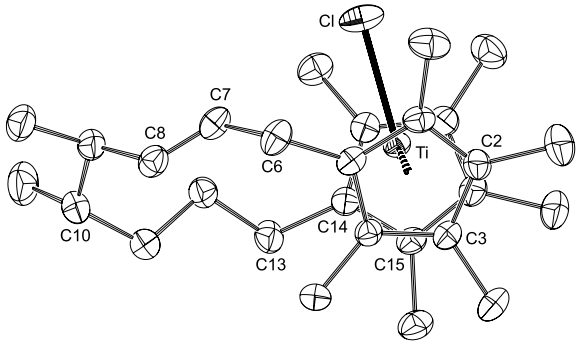

Fig. 4. A view of structure of **4a** along the Cg(1)–Cg(2) direction.

Table 3
Selected bond lengths (Å) and bond angles (°) for **4a**

Bond lengths			
Ti–Cg(1) [a]	2.085(4)	Ti–Cg(2) [a]	2.078(4)
Ti–Cl	2.352(1)	Ti–C(1)	2.426(3)
Ti–C(2)	2.380(4)	Ti–C(3)	2.399(4)
Ti–C(4)	2.407(4)	Ti–C(5)	2.430(3)
Ti–C(14)	2.399(3)	Ti–C(15)	2.407(3)
Ti–C(16)	2.392(3)	Ti–C(17)	2.388(4)
Ti–C(18)	2.429(3)	C_{ring}–C_{Me}	1.492–1.518(6)
C(5)–C(6)	1.512(5)	C(6)–C(7)	1.504(6)
C(7)–C(8)	1.305(6)	C(8)–C(9)	1.497(6)
C(9)–C(10)	1.531(6)	C(10)–C(11)	1.519(6)
C(11)–C(12)	1.526(6)	C(12)–C(13)	1.545(5)
C(13)–C(14)	1.511(5)	C(9)–C(23)	1.532(6)
C(10)–C(24)	1.529(7)		
Bond angles			
Cg(1)–Ti–Cg(2) [a]	142.8(4)	Cl–Ti–Cg(1)	109.1(4)
Cl–Ti–Cg(2)	107.9(4)	C(5)–C(6)–C(7)	117.1(3)
C(6)–C(7)–C(8)	126.8(4)	C(7)–C(8)–C(9)	126.2(4)
C(8)–C(9)–C(10)	114.2(3)	C(9)–C(10)–C(11)	114.7(3)
C(10)–C(11)–C(12)	116.5(4)	C(11)–C(12)–C(13)	111.5(4)
C(12)–C(13)–C(14)	116.6(3)	ϕ [b]	38.7(3)

[a] Cg(1) and Cg(2) are centroids of the C(1–5) and C(14–18) cyclopentadienyl rings, respectively.

[b] Dihedral angle between the least-squares cyclopentadienyl planes.

bon chain without distortion of the tetrahedral angles at the carbon atoms (Table 2). The angle between the least-squares planes of the cyclopentadienyl rings is 37.4(2)° which is close to those in the non-bridged [$TiCl(\eta^5$-$C_5Me_4R)_2$] compounds [16]. The side placement of the five-membered *ansa*-bridge does not affect the position of the cyclopentadienyl rings as the angle between their least-squares planes and the Cg, Ti, Cg′ plane is nearly perpendicular (88.0(5)°). Also, no slippage of the cyclopentadienyl rings occurs in the structure of **1a** as indicated by the cyclopentadienyl-ring slippage angle of only 0.03°. Hence, the factors influencing the structure are some repulsion forces between the chloride ligand and the cyclopentadienyl rings at the open side of the titanocene unit and a steric hindrance between the methyl groups on the inclined side of the titanocene moiety.

Compound **4a** is unsymmetrical because of the presence of one double bond between the C(7) and C(8) carbon atoms within the *ansa*-chain (Fig. 3). The titanocene moiety is opened towards the chlorine atom and the cyclopentadienyl rings adopt a staggered conformation. This conformation allows for a slightly larger angle subtended by cyclopentadienyl least-squares planes than in **1a** (38.7(3) vs. 37.4(2)°). The methyl groups at the hinge position show the largest deviations from the cyclopentadienyl-ring planes (C(21) 0.372(8) and C(25) 0.342(7) Å), while the other methyl groups are deviated at the maximum 0.188(7) Å and the carbon atoms of the *ansa*-chain C(6) and C(13) by 0.168(7) and 0.113(7) Å, respectively. The *ansa*-chain is located in a side position with respect to the Cg(1), Ti, Cg(2) plane as shown in Fig. 4. The shortening of one arm of the chain resulting from the presence of the double bond (C(7)–C(8) 1.305(6) Å) is roughly compensated by more acute tetrahedral angles in the other arm (see Table 3). The torsion angle at the double bond 177.7(3)° and the valence angles at both the sp^3 and sp^2 carbon atoms do not imply any strain.

The solid-state structure of compound **3** is remarkably different from that of the saturated analogue **2** [11]; whereas in **2** the chain carbon atoms are linked in hinge positions of the staggered cyclopentadienyl rings; in **3**, the chain is bound to the carbon atoms of approximately staggered cyclopentadienyl rings in side positions (with respect to the plane defined by the Cg(1), Ti, Cg(2); Figs. 5, 6). The unsaturated *ansa*-chain is further placed strongly asymetrically with respect to the Cl(1), Ti, Cl(2) plane which is at variance with an almost symmetrical placement of the chain in **2** or **4a** (with respect to the plane bisecting the Cg–Ti–Cg angle). A steric repulsion between the two chlorine atoms and the cyclopentadienyl ligands and a higher coordination number of pseudotetrahedrally coordinated Ti(IV) in **3** apparently results in longer Ti–Cl and Ti–C bonds (Table 4) compared to those in **4a** or **1a**

Table 4
Selected bond lengths (Å) and bond angles (°) for **3**

Bond lengths			
Ti–Cg(1) [a]	2.137(3)	Ti–Cg(2) [a]	2.120(3)
Ti–Cl(1)	2.3607(8)	Ti–Cl(2)	2.3517(8)
Ti–C(1)	2.451(2)	Ti–C(2)	2.413(2)
Ti–C(3)	2.436(2)	Ti–C(4)	2.503(2)
Ti–C(5)	2.464(2)	Ti–C(14)	2.422(2)
Ti–C(15)	2.421(2)	Ti–C(16)	2.425(2)
Ti–C(17)	2.478(2)	Ti–C(18)	2.453(2)
C_{ring}–C_{Me}	1.494–1.503(4)	C(5)–C(6)	1.514(3)
C(6)–C(7)	1.511(4)	C(7)–C(8)	1.328(4)
C(8)–C(9)	1.506(4)	C(9)–C(10)	1.545(4)
C(10)–C(11)	1.534(4)	C(11)–C(12)	1.533(4)
C(12)–C(13)	1.535(3)	C(13)–C(14)	1.507(3)
C(13)–C(14)	1.511(5)		
Bond angles			
Cg(1)–Ti–Cg(2) [a]	137.7(2)	Cl(1)–Ti–Cl(2)	92.8(1)
C(5)–C(6)–C(7)	114.9(2)	C(6)–C(7)–C(8)	125.3(3)
C(7)–C(8)–C(9)	124.7(3)	C(8)–C(9)–(10)	115.6(2)
C(9)–C(10)–C(11)	118.3(2)	C(10)–C(11)–C(12)	117.3(2)
C(11)–C(12)–C(13)	113.2(2)	C(12)–C(13)–C(14)	113.9(2)
ϕ [b]	43.8(2)	ω_1 [c]	21.3(2)
ω_2 [d]	22.6(2)		

[a] Cg(1) and Cg(2) are centroids of the C(1–5) and C(14–18) cyclopentadienyl rings, respectively.
[b] Dihedral angle between the least-squares cyclopentadienyl planes.
[c] Dihedral angle between the plane of Cl(1), Ti, and Cl(2) atoms and the least-squares plane defined by the C(1–5) atoms.
[d] Dihedral angle between the plane of Cl(1), Ti, and Cl(2) atoms and the least-squares plane defined by the C(14–18) atoms.

(coordination number 3). Also, the Cg(1)–Ti–Cg(2) angle is more acute and the angle between the least-squares planes of the cyclopentadienyl rings is larger than the corresponding angles in the structure of **4a** for the same reason. On the other hand, all the mentioned values in **3** do not differ from the values found in **2** within the precision of measurement. The carbon atoms of methyl groups in hinge positions C(19) and C(23) are declined from the cyclopentadienyl-ring planes by 0.430(4) and 0.358(4) Å, respectively, whereas the vicinal chain carbon atoms C(6) by 0.268(4) Å and C(13)

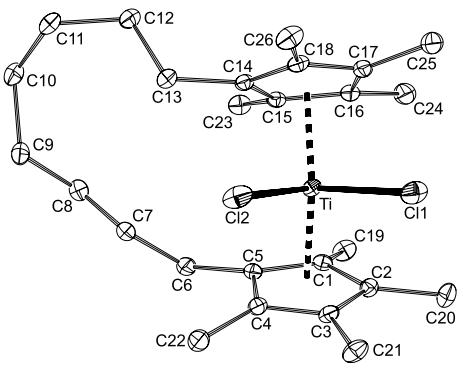

Fig. 5. Molecular structure of **3** (30% probability ellipsoids) with the atom numbering scheme. Hydrogen atoms are omitted.

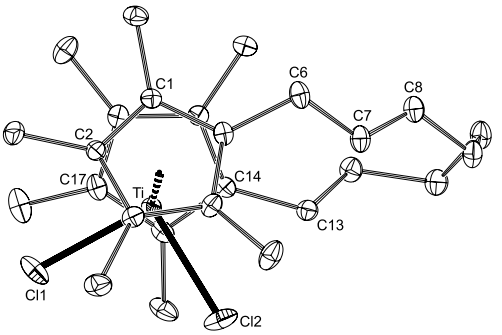

Fig. 6. A view of molecular structure of **3** along the Cg(1)–Cg(2) direction.

by 0.089(4) Å only. The C–C and C=C distances and valence angles in the *ansa*-chain are typical for sp^3 and sp^2 carbon atoms and torsion angle at the double bond 177.7(2)° do not indicate any strain in spite of the asymmetrically placed chain (ring slippage angle 0.06°).

3. Conclusions

Compared to fully substituted titanocene dichlorides without *ansa*-chains the parameters of the titanocene moiety in **3**, particularly the dihedral angle ϕ (43.8(1)°), is close to that of $[TiCl_2(\eta^5\text{-}C_5Me_5)_2]$ (44.6°) [18], smaller than that of $[TiCl_2(\eta^5\text{-}C_5Me_4Ph)_2]$ (45.6°) [14] but larger than ϕ in $[TiCl_2(\eta^5\text{-}C_5Me_4SiMe_3)_2]$ (39.8°) [13]. In the series of titanocene monochlorides the dihedral angles ϕ 37.38° for **1a** and 38.7° for **4a** are somewhat larger than the ϕ angles in $[TiCl(\eta^5\text{-}(C_5Me_5)_2]$ 36.4° [19], 36.6° in $[TiCl(\eta^5\text{-}C_5Me_4Ph)_2]$ [16] and 35.8° in $[TiCl(\eta^5\text{-}C_5Me_4SiMe_3)_2]$ [15]. This shows that the *ansa*-chain has some freedom in mutual rotation and bending of the cyclopentadienyl rings and one may thus suggest that the conformation of the chain is influenced by the requirements of the optimum crystal packing. This is in agreement with combined force field and DFT calculations for compound **2** [8]. A more anisotropic ESR *g*-tensor in **1a** compared to that in **4a** can be accounted for a smaller angle ϕ found in crystal structures, however, the structures from crystal state need not be identical with the structures in toluene glass where the ESR spectra were measured.

4. Experimental

4.1. General data and methods

All operations with titanium complexes were carried out under vacuum in sealed glass devices equipped with breakable seals. A combined device equipped with a pair of quartz cuvettes (10.0 and 1.0 mm, Hellma) and a quartz tube was used for the UV–near infrared (NIR)

and ESR measurements. Crystals for EIMS measurements and melting point (m.p.) determinations were placed in glass capillaries in a glovebox Labmaster 130 (mBraun) under purified nitrogen (concentrations of oxygen and water lower than 2.0 ppm). UV–NIR measurements were performed in a Varian Cary 17D spectrometer in the 340–2000 nm range. ESR spectra were measured in an ERS-220 spectrometer (Centre for Production of Scientific Instruments, Academy of Sciences of GDR, Berlin, Germany) operated by a CU-1 unit (Magnettech, Berlin, Germany) in the X-band. The g-values were determined using an Mn^{2+} standard at $g = 1.9860$ ($M_I = -1/2$ line). A variable temperature unit STT-3 was used for measurements in the -143–23 °C range. EIMS spectra were obtained in a VG-7070E double-focusing mass spectrometer at 70 eV. The crystalline samples in sealed capillaries were opened and inserted into the direct inlet under Ar. The spectra are represented by the peaks of relative abundance higher than 6% and by important peaks of lower intensity. IR spectra were recorded in an air-protecting cuvette on a Nicolet Avatar FTIR spectrometer in the range of 400–4000 cm^{-1}. Samples in KBr pellets were prepared in a glovebox Labmaster 130 (mBraun).

4.2. Chemicals

Solvents THF, hexane, and toluene were dried by refluxing over $LiAlH_4$ and stored as solutions of dimeric titanocene [(μ-η^5:η^5-$C_{10}H_8$)(μ-H)$_2${Ti(η^5-C_5H_5)}$_2$] [20]. Compounds *ansa*-[{η^5:η^5-C_5Me_4CH(Me)CH_2CH_2CH(Me)CH(Me)C_5Me_4}$TiCl_2$] (**1**), *ansa*-[{η^5:η^5-$C_5Me_4(CH_2)_8C_5Me_4$}$TiCl_2$] (**2**), *ansa*-[{η^5:η^5-$C_5Me_4CH_2CH{=}CH(CH_2)_5C_5Me_4$}$TiCl_2$] (**3**), and *ansa*-[{η^5:η^5 - $C_5Me_4(CH_2)_3$CH(Me)CH(Me)CH=CH$CH_2C_5Me_4$}$TiCl_2$] (**4**) were prepared by procedures described previously [11]. Compounds **2** and **3** were obtained by fractional crystallization from their mixture in toluene. The less soluble compound **2** finally contained about 5% of **3** while the final solution of compound **3** contained ca. 5% of **2** according to NMR spectra. Small amount of red crystalline compound **3** was obtained from the latter solution and used for the measurement of EIMS spectra and X-ray diffraction analysis.

4.2.1. Analytical data for *3*

M.p. (dec.) 198 °C. EIMS (180 °C, m/z (relative abundance)): 470 (40), 469 (23), 468 ($M^{+\bullet}$; 55), 435 (32), 434 (35), 433 ($[M-Cl]^+$; 71), 432 (35), 241 (22), 239 (20), 231 (22), 227 (30), 219 (33), 218 (42), 217 (78), 216 (30), 215 (32), 213 (51), 161 (26), 159 (33), 147 (50), 135 (86), 134 (41), 133 (72), 122 (26), 121 (29), 120 (27), 119 (100), 117 (29), 105 (57), 91 (65), 79 (23), 77 (28), 55 (34), 43 (27), 41 (64), 40 (24).

4.3. Preparation of ansa-titanocene monochlorides *1a*, *2a* and *4a*

Magnesium turnings (15 mg, 0.6 mmol) were added to a solution of compounds **1**, **2** or **4** (1.0 mmol, 0.470 g for **1** and **2** or 0.496 g for **4**), respectively, in THF (10 ml) and the mixture was stirred at 60 °C until the initial brown–red colour turned turquoise. Then, the solvent was distilled off under vacuum and the residue was extracted with hexane. The extract was concentrated to ca. 2.0 ml, a yellowish-green solution was poured away from a separated green solid residue and the solid was recrystallized from hexane to give turquoise crystals of the products.

4.3.1. *ansa-[{η^5:η^5-C_5Me_4CH(Me)CH_2CH_2CH(Me)CH(Me)C_5Me_4}TiCl] (1a)*

Yield: 0.374 g (86%). M.p. (dec.) 220 °C. EIMS (90 °C, m/z (relative abundance)): 438 (15), 437 (46), 436 (38), 435 ($M^{+\bullet}$; 100), 434 (15), 433 (12), 400 (6), 398 (10), 397 (16), 396 (14), 395 (32), 394 (9), 393 (14), 391 (8), 288 (8), 286 (19), 241 (8), 234 (6), 233 (9), 232 (20), 231 (20), 230 (14), 229 (25), 228 (16), 227 (61), 226 (11), 225 (9), 217 (7), 215 (7), 213 (14), 192 (6), 191 (7), 149 (28), 147 (7), 133 (14), 119 (7), 105 (8), 91 (9), 69 (6), 57 (8), 55 (15), 43 (10), 41 (15). IR (KBr, cm^{-1}): 2953 (vs), 2912 (vs,b), 2858 (s), 2815 (s), 1448 (vs), 1375 (s), 1358 (m), 1140 (w), 1023 (m), 995 (w), 867 (w), 818 (w), 772 (vw), 688 (vw), 669 (w), 569 (vw), 473 (vw), 420 (vw). ESR (toluene, 22 °C): $g = 1.948$, $H = 23.0$ G. ESR (toluene, -140 °C): $g_1 = 1.998$, $g_2 = 1.982$, $g_3 = 1.865$, $g_{av} = 1.948$. UV–vis (toluene): 360 (sh) ≫ 585 > 670 (sh).

4.3.2. *ansa-[{η^5:η^5-$C_5Me_4(CH_2)_8C_5Me_4$}TiCl] (2a)*

Yield: 0.361 g (83%). M.p. 227 °C. EIMS (90 °C, m/z (relative abundance)): 438 (15), 437 (46), 436 (38), 435 ($M^{+\bullet}$; 100). IR (KBr, cm^{-1}): 2964 (vs), 2916 (vs,b), 2900 (s), 2874 (m), 1486 (m), 1443 (s), 1411 (m), 1373 (s), 1072 (w), 1026 (s), 664 (w), 492 (w), 438 (s), 421 (w). ESR (toluene, 22 °C): $g = 1.952$, $H = 16$ G. ESR (toluene, -140 °C): $g_1 = 1.998$, $g_2 = 1.983$, $g_3 = 1.882$, $g_{av} = 1.9542$. UV–vis (toluene): 360(sh) ≫ 590 > 670 (sh).

4.3.3. *ansa-[{η^5:η^5-$C_5Me_4(CH_2)_3$CH(Me)CH(Me)CH=CH$CH_2C_5Me_4$}TiCl] (4a)*

Yield: 0.421 g, 91%. M.p. (dec.) 189 °C. EIMS (90 °C, m/z (relative abundance)): 464 (14), 463 (49, 462 (34), 461 ($M^{+\bullet}$; 100), 460 (16), 459 (15), 421 (6), 241 (6), 227 (10), 219 (15), 218 (14), 217 (34), 216 (8), 215 (12), 213 (21), 135 (6), 41 (6). IR (KBr, cm^{-1}): 2955 (vs), 2919 (vs,b), 2878 (s), 2857 (m), 1453 (s), 1378 (s), 1071 (m), 1024 (m), 990 (s), 791 (m), 730 (w), 429 (m). ESR (toluene, 22 °C): $g = 1.955$, $H = 10$ G. ESR (toluene, -140 °C): $g_1 = 1.999$, $g_2 = 1.982$, $g_3 = 1.893$;

Table 5
Crystal data and structure refinement parameters for **1a**, **3** and **4a**

Compound	**1a**	**3**	**4a**
Empirical formula	$C_{26}H_{40}ClTi$	$C_{26}H_{38}Cl_2Ti$	$C_{28}H_{42}ClTi$
Formula weight	435.95	469.36	461.97
Temperature (K)	293	105	293
Crystal system	Monoclinic	Monoclinic	Monoclinic
Space group	$P2_1/m$ (no. 11)	$P2_1/c$ (no. 14)	$P2_1/c$ (no. 14)
Unit cell dimensions			
a (Å)	8.2650(2)	14.8574(4)	12.550(1)
b (Å)	16.4070(4)	8.4305(3)	11.774(1)
c (Å)	8.7970(2)	18.9273(6)	17.413(1)
β (°)	101.134(1)	93.576(2)	92.421(5)
V (Å^3)	1170.45(5)	2366.1(1)	2570.6(4)
Z	2	4	4
D_{calc} (g cm^{-3})	1.305	1.318	1.194
μ (Mo–K$_\alpha$) (mm^{-1})	0.493	0.598	0.449
$F(000)$	494	1000	996
Crystal colour	Turquoise	Red	Turquoise
Crystal size (mm^3)	$0.50\times0.25\times0.20$	$0.38\times0.25\times0.25$	$0.63\times0.30\times0.15$
θ Range (°)	3.10–27.49	3.24–27.51	4.02–25.03
Index ranges	$0\le h\le10$, $0\le k\le21$, $-11\le l\le11$	$0\le h\le19$, $0\le k\le10$, $-24\le l\le24$	$0\le h\le14$, $0\le k\le-14$, $-20\le l\le20$
Number of unique diffractions	2769	5380	4439
Number of observed diffractions [a]	2467	4145	3238
Number of parameters	211	414	397
Weighting scheme: w_1, w_2 [b]	0.100, 0.000	0.019, 3.336	0.032, 2.709
$R(F^2)$, $wR(F^2)$ (all data) [c]	0.041, 0.130	0.076, 0.099	0.092, 0.134
$R(F^2)$, $wR(F^2)$ (observed diffractions) [c]	0.035, 0.124	0.047, 0.085	0.058, 0.115
S (all data) [d]	1.10	1.08	1.09
$(\Delta/\rho)_{max}$ (e Å^{-3})	0.34, and −0.40	0.32, and −0.41	0.22, and −0.26

[a] Diffractions with $I_o > 2\sigma(I_o)$.
[b] Weighting scheme: $w=[\sigma^2(F_o^2)+(w_1P)^2+w_2P]^{-1}$, where $P=1/3[\max(F_o^2)+2F_c^2]$.
[c] $R(F)=\Sigma\big||F_o|-|F_c|\big|/\Sigma|F_o|$, $wR(F^2)=[\Sigma(w(F_o^2-F_c^2)^2)/(\Sigma w(F_o^2)^2)]^{1/2}$.
[d] Goodness-of-fit $=[\Sigma(w(F_o^2-F_c^2)^2)/(N_{diffrs}-N_{params})]^{1/2}$.

$g_{av}=1.958$. UV–vis (toluene): 360 (sh) $\gg$ 580 $>$ 670 (sh).

4.4. Crystal structure analyses of *1a*, *3* and *4a*

Turquoise prismatic crystals of complexes **1a** and **4a**, and a fragment of a red crystal of **3** were inserted into Lindemann glass capillaries in a glove box. All diffraction data were collected in an image plate Nonius KappaCCD diffractometer. The structures were solved by direct methods (SIR-92, [21]) and refined by full-matrix least-squares on F^2 (SHELXL-97 [22]). Relevant crystallographic data are given in Table 5; particular details about the structure solution follow:

4.4.1. Compound *1a*

All non-hydrogen atoms were refined anisotropically. Hydrogen atoms were identified on difference electron density maps and isotropically refined with the exception of the methyl hydrogen atoms on the disordered C(14) atom which were included in calculated positions [C–H 0.96 Å, $U_{iso}(H)=1.2\ U_{eq}(C)$].

4.4.2. Compound *3*

The non-hydrogen atoms were refined anisotropically. Hydrogen atoms were located on difference electron density maps and refined with isotropic thermal motion parameters.

4.4.3. Compound *4a*

The non-hydrogen atoms were refined anisotropically. Hydrogen atoms were found on difference electron density maps and refined with isotropic thermal motion parameters $U_{iso}(H)$ assigned to 1.2 (methylene and methine) or 1.5 (methyl) times the thermal motion parameter $U_{eq}(C)$ of their parent carbon atoms.

5. Supplementary material

Crystallographic data for the structural analysis have been deposited with the Cambridge Crystallographic Data Centre, CCDC nos. 166326, 166327 and 166325 for compounds **1a**, **3** and **4**, respectively. Copies of this information may be obtained free of charge from The

Director, CCDC, 12 Union Road, Cambridge, CB2 1EZ, UK (Fax: +44-1223-336033; e-mail: deposit@ccdc.cam.ac.uk or www: http://www.ccdc.cam.ac.uk).

Acknowledgements

This investigation was supported by the Grant Agency of Academy of Sciences of the Czech Republic (project no. A404004), and is a part of a long-term research plan of the Faculty of Sciences, Charles University (MSM 11310001). Grant Agency of the Czech Republic sponsored access to Cambridge Structure Database (grant no. 203/99/0067).

References

[1] (a) C. Janiak, in: A. Togni, R.L. Halterman (Eds.), Metallocenes, vol. 2, Wiley–VCH, Weinheim, 1998, p. 547 (chap. 9); (b) W. Kaminsky, M. Arndt, Adv. Polym. Sci. 127 (1997) 143; (c) H.-H. Brintzinger, D. Fischer, R. Mühlhaupt, B. Rieger, R. Waymouth, Angew. Chem. Int. Ed. Engl. 34 (1995) 1143.
[2] G.W. Coates, R.M. Waymouth, Science 267 (1995) 217.
[3] R.L. Halterman, in: A. Togni, R.L. Halterman (Eds.), Metallocenes, vol. 1, Wiley–VCH, Weinheim, 1998, p. 455 (chap. 8).
[4] M.E. Huttenloch, J. Diebold, U. Rief, H.H. Brintzinger, Organometallics 11 (1992) 3600.
[5] K.-L. Gibis, G. Helmchen, G. Huttner, L. Zsolnai, J. Organomet. Chem. 445 (1993) 181.
[6] (a) M.J. Burk, S.L. Colletti, R.L. Halterman, Organometallics 10 (1991) 2998; (b) T.K. Hollis, A.L. Rheingold, N.P. Robinson, J. Whelan, B. Bosnich, Organometallics 11 (1992) 2812.
[7] G. Erker, C. Mollenkopf, M. Grehl, R. Fröhlich, C. Krüger, R. Noe, M. Riedel, Organometallics 13 (1994) 1950.
[8] T. Jödicke, F. Menges, G. Kehr, G. Erker, U. Höweler, R. Fröhlich, Eur. J. Inorg. Chem. (2001) 2097.
[9] W. Röll, L. Zsolnai, G. Huttner, H.H. Brintzinger, J. Organomet. Chem. 322 (1987) 65.
[10] H. Lang, D. Seyferth, Organometallics 10 (1991) 347.
[11] M. Horáček, P. Štěpnička, R. Gyepes, I. Císařová, I. Tišlerová, J. Zemánek, J. Kubišta, K. Mach, Chem. Eur. J. 6 (2000) 2397.
[12] T.H. Waren, G. Erker, R. Fröhlich, B. Wibbeling, Organometallics 19 (2000) 127.
[13] K. Mach, J.B. Raynor, J. Chem. Soc. Dalton Trans. (1992) 683.
[14] W.W. Lukens, M.R. Smith III, R.A. Andersen, J. Am. Chem. Soc. 118 (1996) 1719.
[15] M. Horáček, M. Polášek, V. Kupfer, U. Thewalt, K. Mach, Collect. Czech. Chem. Commun. 64 (1999) 61.
[16] M. Horáček, R. Gyepes, I. Císařová, M. Polášek, V. Varga, K. Mach, Collect. Czech. Chem. Commun. 61 (1996) 1307.
[17] J.W. Lauher, R. Hoffmann, J. Am. Chem. Soc. 98 (1976) 1729.
[18] T.C. McKenzie, R.D. Sanner, J.E. Bercaw, J. Organomet. Chem. 102 (1975) 457.
[19] J.W. Pattiasina, H.J. Heeres, F. van Bolhuis, A. Meetsma, J.H. Teuben, A.L. Spek, Organometallics 6 (1987) 1004.
[20] H. Antropiusová, A. Dosedlová, V. Hanuš, K. Mach, Transition Met. Chem. (London) 6 (1981) 90.
[21] A. Altomare, M.C. Burla, M. Camalli, G. Cascarano, C. Giacavazzo, A. Guagliardi, G. Polidori, J. Appl. Crystallogr. 27 (1994) 435.
[22] G.M. Sheldrick, SHELXL-97, Program for Crystal Structure Refinement from Diffraction Data, University of Göttingen, Göttingen, Germany, 1997.